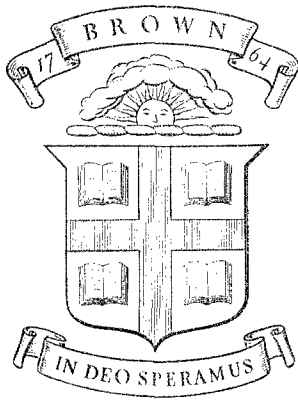


BU
ARPA-E-46



Division of Engineering
BROWN UNIVERSITY
PROVIDENCE, R. I.

INFLUENCE OF STRAIN-HARDENING AND
STRAIN-RATE SENSITIVITY ON THE
PERMANENT DEFORMATION OF IMPULSIVELY
LOADED RIGID-PLASTIC BEAMS

N. JONES

3 cop
1 - R
1 - M Zukas
1 - Mr. C. Allen

AD657129

20060110153

Department of Defense
Advanced Research Projects Agency
Contract SD-86
Materials Research Program

ARPA E46

July 1967

BU
ARPA-E-46

INFLUENCE OF STRAIN-HARDENING AND STRAIN-RATE SENSITIVITY ON THE
PERMANENT DEFORMATION OF IMPULSIVELY LOADED RIGID-PLASTIC BEAMS*

by


Norman Jones

TECHNICAL LIBRARY
BLDG 313
ABERDEEN PROVING GROUND MD.
STEAP-TL

Division of Engineering
Brown University
Providence, Rhode Island

July 1967

* The research reported here was supported by the Advanced Research Projects Agency, Department of Defense, under Contract Number SD-86.



U

INFLUENCE OF STRAIN-HARDENING AND STRAIN-RATE SENSITIVITY ON THE
PERMANENT DEFORMATION OF IMPULSIVELY LOADED RIGID-PLASTIC BEAMS

by

Norman Jones

Abstract

A simple method is presented for estimating the combined influence of strain-hardening and strain-rate sensitivity on the permanent deformation of rigid-plastic structures loaded dynamically. A study is made of the particular case of a beam supported at the ends by immovable frictionless pins and loaded with a uniform impulse. The results of this work indicates that considering strain-hardening alone when appropriate or strain-rate sensitivity alone gives permanent deformations which are similar to those predicted by an analysis retaining both effects simultaneously.

Notation

D	strain-rate sensitivity coefficient defined in equation (38)
E	modulus of elasticity
H	thickness of beam
G_k, J_k	coefficients given by equations (64) and (65)
L	semi-length of beam
M	longitudinal bending moment per unit width of beam
M_o	$\sigma_o H^2/4$
N	axial force per unit width of beam
N_o	$\sigma_o H$
Q	shear force per unit width of beam
R	radius of curvature of mid-plane of beam
T, T_f	time
V_o	initial velocity of beam
b	$-k \sin\phi$
c_R, c_H	constants defined in equations (61), (76)
k	uniform distributed pressure per unit area of undeformed beam
m	M/M_o
n	N/N_o
n_A, n_C, n_F n_H, n_o, n_R	dimensionless membrane forces defined by equations (80, 84, 79, 74, 85, 59)
p	strain-rate sensitivity coefficient defined in equation (38)
q	$-k \cos\phi$

Notation (continued)

r	ratio of the slopes of the elastic and plastic portions of the stress-strain curve
s	distance measured along deformed mid-plane
t	time
t_1	duration of first stage of motion
t_0	t_1/L^2
t_f	time at which beam reaches its permanent position
u, w	displacements defined in Fig. 1
w_m	maximum permanent transverse displacement
x	distance defined in Fig. 1 (measured from beam center)
y	distance measured from left-hand support of beam
z	distance defined in Fig. 1
α	$\frac{2V_0 H^{1/p}}{DL^2}$
β	$\sum_{k=1,3,5}^{\infty} \frac{1}{k^4}$
γ	vH^2/L^2
δ_1	$V_0 t_1$
ϵ	axial strain of mid-plane
ϵ_z	axial strain at distance z from mid-plane
$\bar{\epsilon}$	defined by equation (77)
η	$\{w'^2 + (1 + u')^2\}^{1/2}$
κ	curvature

Notation (continued)

λ	$\frac{\mu V_o^2 L^2}{M_o H}$
μ	mass per unit length of beam
ν	$\frac{E}{r \sigma_o}$
ρ	radius of a traveling hinge
σ	stress
σ_o	yield stress in simple tension
τ	$\frac{\mu V_o L^2}{6M_o}$
ϕ	slope of the mid-plane of beam
ψ	$\sum_{k=1,3,5}^{\infty} \frac{1}{k^3}$
Δ	δ_1/H
$(\dot{\quad})$	$\frac{\partial}{\partial t} (\quad)$
$(\quad)'$	$\frac{\partial}{\partial x} (\quad)$
[]	difference between the values of the considered quantity on either side of a traveling hinge

1. Introduction

Parkes [1] examined the permanent deformation of cantilever beams loaded dynamically and observed that a simple rigid, perfectly plastic analysis overestimated considerably the final maximum deflections. The rather significant discrepancies between experimental results and theoretical predictions were accounted for by considering, in an approximate manner, the influence of strain-rate sensitivity on the dynamic plastic bending moment. Ting [2] analyzed a rigid, perfectly plastic cantilever beam loaded dynamically at its tip and indicated that geometry changes when treated rigorously were responsible for part of the discrepancies between Parke's theory and experiments [1]. Bodner and Symonds [3,4] conducted more exhaustive tests on cantilever beams loaded dynamically and observed that strain-hardening was not very important while strain-rate sensitivity must be considered throughout the entire deformation history. Ting and Symonds [5] analyzed the plastic deformation of a cantilever beam with an attached tip mass which was subjected to a rapid transverse velocity change at the base and found that, if the strain-rate dependence of yield stress and geometry changes were considered, then the predictions showed good agreement with corresponding experimental results.

Parkes [6] developed the earlier theoretical work of Lee and Symonds [7] in order to describe the behavior of a rigid, perfectly plastic encastré beam struck transversely at any point on the span. The predictions were compared with some experimental values recorded on steel, brass, and duralumin beams, the supports of which were prevented from rotating but were free to move axially. It was found subsequently that better agreement between experimental results and theoretical predictions was obtained when the dynamic plastic

bending moment was calculated using a yield stress given by Manjoine [8] corresponding to a mean value of strain-rate. Symonds and Mentel [9] examined the influence of axial restraints on beams loaded impulsively and predicted final deformations which were considerably smaller than those expected from the corresponding simple beam solution when deflections of the order of the beam depth, or larger, were permitted. Humphreys [10] conducted some experimental tests and confirmed this prediction, indicating that the simple theory is only useful for maximum deflections of magnitudes up to the order of the beam thickness. In reference [11] Florence and Firth report the results of some experiments in which pinned and clamped beams without axial restraints were subjected to uniformly distributed impulses large enough to cause considerable plastic deformation. It was found that a rigid-plastic analysis, which disregarded strain-rate effects entirely, but included strain-hardening in an approximate manner during the second stage of motion, gave somewhat better agreement with the experimental results than a simple rigid-plastic analysis.

Recently, Nonaka [12] studied the behavior of clamped beams, with restraints against axial displacements at the supports, when an attached mass in the center was subjected to large transverse dynamic loads. It was observed that, except when the attached mass was small, a major portion of the deformation occurred under a one degree of freedom mode in which the two halves of the beam rotate about the supports. Consequently, the mode approximation method of Martin and Symonds [13], which has been used by Symonds [14] to study a cantilever beam loaded impulsively, was utilized in order to estimate the effects of strain-rate sensitivity, elasticity, and load duration on the final deformation.

Apart from the numerical work of Witmer, Balmer, Leech and Pian [15] the combined influence of strain-hardening and strain-rate sensitivity on the permanent deformations of rigid-plastic beams with immovable supports arising from uniform impulses has not been studied and is taken, therefore, as the subject of interest in this article. In order to retain the attractive simplicity of rigid-plastic analyses, an attempt is made to develop a method which is mathematically simple yet at the same time sufficiently accurate to be worthwhile exploring the possibility of using it to analyze the behavior of more complex structures.

2. General Equations

An expression for the axial strain at any position in a beam is derived in this section in terms of the membrane or axial strain and curvature of the mid-surface. The equilibrium equations for a uniform beam loaded dynamically are then derived and recast into a form convenient for later use.

2.1 Axial Strain

It may be shown that

$$ds = \eta dx \quad (1)$$

where

$$\eta = \{w'^2 + (1 + u')^2\}^{1/2}, \quad (2)$$

$$(\)' = \frac{\partial}{\partial x} (\),$$

and the remaining quantities are defined in Fig. 1.

Thus,

$$\epsilon = \eta - 1 \quad (3)$$

is the axial strain of the mid-surface of the beam which becomes

$$\epsilon = u' + \frac{w'^2}{2} + \dots, \quad (4)$$

when η is expanded.

The radius of curvature "R" of the mid-surface of the beam is, by definition,

$$R = \frac{\partial s}{\partial \phi},$$

which, using the geometrical identity

$$\tan \phi = \frac{-w'}{1+u'}$$

from Fig. 1(a) and equation (1) yields

$$\frac{1}{R} = \frac{-w''(1+u') + w'u''}{\eta^3} \quad (5)$$

If it is assumed that plane cross-sections remain plane during deformation and merely rotate about the mid-surface of the beam, then it may be shown that the axial strain at distance "z" is

$$\epsilon_z = \epsilon + z\kappa \quad (6)$$

where

$$\kappa = \frac{1}{R} + \epsilon \quad (7)$$

and z is defined in Fig. 1(b).

2.2 Equilibrium Equations

The equations of equilibrium for the element of the beam illustrated in Fig. 1(c) can be written in the form

$$\frac{\partial N}{\partial x} - \frac{Q\eta}{R} - \mu\ddot{u}\eta\cos\phi + \mu\ddot{w}\eta\sin\phi + b\eta = 0 \quad (8)$$

$$\frac{\partial Q}{\partial x} + \frac{N\eta}{R} + \mu\ddot{u}\eta\sin\phi + \mu\ddot{w}\eta\cos\phi + q\eta = 0 \quad (9)$$

$$\frac{\partial M}{\partial x} + Q\eta = 0 \quad (10)$$

provided any rotatory inertia effects are ignored and

$$\dot{(\quad)} = \frac{\partial}{\partial t} (\quad) .$$

In order to simplify the theoretical analyses of beams and strings loaded dynamically, the displacement u and acceleration \ddot{u} are usually disregarded [9, etc.]. Thus, let

$$u = u' = \ddot{u} = 0 \quad (11)$$

which allows equations (2) and (4) to be written

$$\eta = (1 + w'^2)^{1/2} \quad (12)$$

and

$$\epsilon = \frac{w'^2}{2} , \quad (13)$$

respectively.

If attention is restricted henceforth to small strains, then

$$\eta = 1 , \quad \sin\phi = -w' , \quad \cos\phi = 1 ,$$

and equations (5) and (7) give

$$\kappa = -w'' \quad (14)$$

Equations (8)-(10) may now be rewritten

$$\frac{\partial N}{\partial x} + Qw'' - \mu\ddot{w}w' + kw' = 0 \quad (15)$$

$$\frac{\partial Q}{\partial x} - Nw'' + \mu\ddot{w} - k = 0 \quad (16)$$

$$\frac{\partial M}{\partial x} + Q = 0 \quad (17)$$

If equation (17) is used to eliminate Q from equations (15) and (16), and the two remaining equations combined, then

$$\frac{d^2M}{dx^2} = -k + \mu\ddot{w} - \frac{d}{dx}(w'N) \quad (18)$$

when disregarding the $w'w'' \frac{\partial M}{\partial x}$ term.

Using $n = N/N_0$, and $m = M/M_0$, equation (18) becomes

$$\frac{dm}{dx} = - \int_0^x \frac{k dx}{M_0} + \int_0^x \frac{\mu\ddot{w} dx}{M_0} - \frac{4w'n}{H} \quad (19)$$

The first term on the right hand side of equation (19) is due to an external load k , the second term $\mu\ddot{w}$ is an inertia force while the last term containing w' introduces the membrane forces arising from axial restraints.

3. Yield Condition

It is indicated in Fig. 2 that an exact yield curve relating the dimensionless bending moment m and membrane force n according to the Tresca shear stress criterion lies everywhere inside a square having sides of magnitude 2, while a square with sides of length 1.236 lies everywhere inside the exact yield curve. In order to estimate the accuracy of this approximate linear yield condition, which can be selected to bound the exact

yield condition, as illustrated in Fig. 2, the particular case of a rigid, perfectly plastic beam loaded impulsively will be studied and the results compared with the final deformations predicted by Symonds and Mentel [9], who used an exact yield curve.

4. Rigid, Perfectly Plastic Beam Subjected to a Uniformly Distributed Impulse

4.1 Simple Bending Solution

The equilibrium equation (19) for this case becomes

$$\frac{d^2m}{dx^2} = \frac{\mu}{M_0} \frac{\partial^2 w}{\partial t^2} \quad (20)$$

if the beam is unloaded ($k = 0$) and there are no axial restraints ($w' = 0$) against deformation.

In accord with experimental evidence and previous analyses, it is assumed that two traveling hinges, each of radius $|\rho(t)|$, originate from the supports at $t = 0$ and travel inwards towards the center of the beam during a first phase, while throughout a second stage, they remain stationary at $x = 0$ until all the initial kinetic energy is dissipated as plastic work.

First Stage

A velocity profile,

$$\dot{w} = V_0 \quad \text{for} \quad 0 \leq x \leq \rho(t) \quad (21)$$

and

$$\dot{w} = \frac{V_0(L-x)}{L-\rho} \quad \text{for} \quad \rho(t) \leq x \leq L, \quad (22)$$

where V_0 is the initial uniform velocity of the beam, is consistent with the normality requirement associated with the yield condition $m = 1$.

If the time derivative of (22) is substituted into (20) and the resulting expression integrated twice with respect to x , one obtains

$$\frac{\mu V_0}{3M_0} (L - \rho)\dot{\rho} + 1 = 0, \quad (23)$$

for a beam which is simply supported at its ends. Integrating (23) with respect to time yields

$$t = \frac{\tau}{L^2} (L^2 - 2L\rho + \rho^2), \quad (24)$$

where

$$\tau = \frac{\mu V_0 L^2}{6M_0} \quad (25)$$

and the requirement that $\rho = L$ when $t = 0$ has been satisfied.

The maximum displacement at the center of the beam at the end of the first stage is $V_0 \tau$.

Second Stage

If a linear velocity profile of the form

$$\dot{w} = \dot{w}(t) \frac{(L - x)}{L} \quad (26)$$

is selected for the second stage, then it may be shown, using (20) and (26) and matching the displacements and velocities at $t = \tau$ with those at the end of the first stage, that

$$\frac{w_m}{H} = \frac{\lambda}{3}, \quad (27)$$

where

$$\lambda = \frac{\mu V_0^2 L^2}{M_0 H} \quad (28)$$

and w_m is the permanent displacement at the center of the beam.

Equation (27) is the same result as equation (4) of reference [9].

4.2 Solution with Axial Restraints

The influence of membrane forces, which arise due to axial restraints, must now be included in the equilibrium equations. Thus, equation (19) becomes

$$\frac{dm}{dx} = \int_0^x \frac{\mu}{M_0} \frac{\partial^2 w}{\partial t^2} dx - \frac{4n}{H} \frac{\partial w}{\partial x} \quad (29)$$

First Stage

If the mechanism of deformation for this case is assumed to be similar to that for the previous one, then the velocity profile is given by equations (21) and (22), and when $0 \leq x \leq \rho$.

$$w = V_0 t \quad (30)$$

while

$$w = V_0 t(x) + \int_{t(x)}^t \frac{\partial w}{\partial t} dt, \quad \text{if } \rho \leq x \leq L \quad (31)$$

Since one might expect bending moments to dominate over the action of membrane forces during the first stage, then the form of the time function $t(\rho)$ for $w' \neq 0$ should be somewhat similar to equation (24) which was obtained by disregarding w' in (19). Therefore, it is assumed that,

$$t(\rho) = t_0(L^2 - 2L\rho + \rho^2), \quad (32)$$

where t_0 is a constant to be determined later.

It may be shown using equations (21, 22, 30, 31, 32) that

$$w' = 0, \quad \text{when} \quad 0 \leq x \leq \rho \quad (33)$$

and

$$w' = 2V_o t_o (\rho - x), \quad \text{if} \quad \rho \leq x \leq L. \quad (34)$$

Equation (29) can be rewritten with the aid of (22) and (34) in the form,

$$\frac{dm}{dx} = \frac{\mu V_o \dot{\rho}}{M_o (L-\rho)^2} \left(Lx - \frac{x^2}{2} - L\rho + \frac{\rho^2}{2} \right) - \frac{8V_o t_o}{H} (\rho - x), \quad (35)$$

provided $\rho \leq x \leq L$, $n = 1$ and $0 \leq m \leq 1$.

Integrating (35) gives

$$m = \frac{\mu V_o \dot{\rho}}{M_o (L-\rho)^2} \left(\frac{Lx^2}{2} - \frac{x^3}{6} - L\rho x + \frac{\rho^2 x}{2} + \frac{L\rho^2}{2} - \frac{\rho^3}{3} \right) - \frac{8V_o t_o}{H} \left(\rho x - \frac{x^2}{2} - \frac{\rho^2}{2} \right) + 1, \quad (36)$$

where the constant of integration has been determined from the requirement that $m = 1$ at $x = \rho$, which in turn can be obtained by solving equation (29) using (21) and (33).

Now for a beam which is supported at pinned ends, $m = 0$ at $x = L$.

Thus (36) gives

$$- \frac{\mu V_o}{2M_o t_o (L-\rho)^3} \left(\frac{L^3}{3} - L^2\rho + L\rho^2 - \frac{\rho^3}{3} \right) - \frac{8V_o t_o}{H} \left(\rho L - \frac{L^2}{2} - \frac{\rho^2}{2} \right) + 1 = 0$$

which, when $\rho = 0$, yields

$$\frac{\delta_1}{H} = \frac{1}{8} \left\{ -1 + \left(1 + \frac{8\lambda}{3} \right)^{1/2} \right\},$$

where $\delta_1 = V_o t_1$ is the maximum deflection ($x = 0$) at the end of the first stage, and from (32), $t_1 = t_o L^2$, when $\rho = 0$.

Second Stage

If a linear velocity profile of the form described by equation (26) is selected for the second stage, then it is straightforward to show, when using the yield condition illustrated in Fig. 2, that the final displacement of the beam at $x = 0$ is

$$\frac{w_m}{H} = \frac{1}{4} \left[\left\{ \frac{1}{2} + 2\lambda + \frac{1}{2} \left(1 + \frac{8\lambda}{3} \right)^{1/2} \right\}^{1/2} - 1 \right] \quad (37)$$

The final deflections at the center of rigid, perfectly plastic beams loaded with uniformly distributed impulses are given by equations (27) and (37) and compared in Fig. 3 with the results of Symonds and Mentel [9]. It is evident that the "upper" and "lower" bounds lie between the two predictions of Symonds and Mentel [9] with and without a string phase, while the deflections forecasted by the simple bending solution given by equation (27) are considerably larger even for very small values of λ . Strictly speaking, the curves designated "upper" and "lower" bounds in Fig. 3 are not upper and lower bounds in the accepted sense since they are based solely on the fact that the deflections designated "upper" bound were calculated using a yield surface which lay on or outside the exact one, while those termed "lower" bound were evaluated using a yield surface which lay everywhere on or inside the exact one.

5. Constitutive Equations

5.1 Strain-Rate Sensitivity

It is well known that the initial yield stress [8, 16, etc.] of many materials increases with increase of strain-rate and that, furthermore, it is important to take account of this effect when analyzing the dynamic

behavior of cantilevers and beams [4,17]. Cowper and Symonds [18] observed that a constitutive equation of the form

$$\frac{\sigma}{\sigma_0} = 1 + \left(\frac{\dot{\epsilon}}{D}\right)^{1/p} \quad (38)$$

could be fitted to the data of Manjoine [8] provided $D = 40.4 \text{ sec.}^{-1}$ and $p = 5$.

On account of its attractive simplicity, the constitutive equation (38) has been used successfully by a number of authors to solve a variety of problems [5,19,20].

If an element of the beam illustrated in Fig. 1 is made from a rigid, rate-sensitive material described by the constitutive equation (38), then it may be shown that

$$\begin{aligned} m = 1 - \left\{ n - \frac{\left(\dot{\epsilon} + \frac{H}{2} \dot{\kappa}\right)^{\frac{p+1}{p}} + \left(\frac{H}{2} \dot{\kappa} - \dot{\epsilon}\right)^{\frac{p+1}{p}}}{HD^{1/p} \dot{\kappa} \frac{(p+1)}{p}} \right\}^2 + \\ + \frac{4p}{H^2 \dot{\kappa}^2 D^{1/p} (2p+1)} \left\{ \left(\dot{\epsilon} + \frac{H}{2} \dot{\kappa}\right)^{\frac{2p+1}{p}} + \left(\frac{H}{2} \dot{\kappa} - \dot{\epsilon}\right)^{\frac{2p+1}{p}} \right\} - \\ - \frac{4p\dot{\epsilon}}{H^2 \dot{\kappa}^2 D^{1/p} (p+1)} \left\{ \left(\dot{\epsilon} + \frac{H}{2} \dot{\kappa}\right)^{\frac{p+1}{p}} - \left(\frac{H}{2} \dot{\kappa} - \dot{\epsilon}\right)^{\frac{p+1}{p}} \right\} \quad (39) \end{aligned}$$

provided plane cross-sections remain plane and during deformation merely rotate about the mid-surface of the beam, and that the directions of m and n correspond to those of M and N in Fig. 1.

When $m = 0$ and $\dot{\kappa} = 0$, it may be shown that

$$n = 1 + \left(\frac{\dot{\epsilon}}{D}\right)^{1/p}, \quad \text{with } \dot{\epsilon} \geq 0 \quad (40)$$

while, for $n = 0$ and $\dot{\epsilon} = 0$,

$$m = 1 + \frac{2p}{2p+1} \left(\frac{H\dot{\kappa}}{2D}\right)^{1/p}, \quad \text{with } \dot{\kappa} \geq 0 \quad (41)$$

In order to simplify the rather complicated constitutive equation (39), let us proceed in a manner somewhat similar to that described previously in section 3 for the rigid, perfectly plastic case. It is assumed that a linearized yield curve will grow as illustrated in Fig. 4(a) such that the behavior suggested by (40) occurs along A'B' with $0 \leq m \leq 1$, while equation (41) describes the behavior of C'D' with $0 \leq n \leq 1$.

Perrone [20,21] has shown, for some simple structures loaded impulsively and made from a strain-rate sensitive material, that excellent agreement with exact solutions may be obtained when utilizing a strain-rate insensitive material with a constant yield stress equal to the initial dynamic yield stress. This observation permits considerable simplification of subsequent analyses but is only valid for large values of p (4 or 5) when most of the kinetic energy is dissipated before the stress-strain-rate point departs appreciably from its initial position.

5.2 Strain Hardening

Cowper and Symonds [18] and others [11, etc.] have suggested a linear strain-hardening relation of the form,

$$\frac{\sigma}{\sigma_0} = 1 + \frac{E\epsilon}{\sigma_0 r}, \quad (42)$$

where "E" is the Elastic Modulus and "r" may be interpreted as the ratio of the slopes of the elastic and plastic portions of the stress-strain curve.

If plane cross-sections are assumed to remain plane and merely rotate about the mid-surface of the beam during deformation, then it may be shown, using equation (42), that

$$m = 1 - (n - \nu\epsilon)^2 + \frac{\nu H\kappa}{3} , \quad (43)$$

provided "m" and "n" act in the directions of "M" and "N" indicated in Fig. 1, and $\nu = \frac{E}{\sigma_0 r}$.

When $m = \kappa = 0$, it may be shown that

$$n = 1 + \nu\epsilon , \quad \text{provided } \epsilon \geq 0 , \quad (44)$$

while, if $n = \epsilon = 0$, and $\kappa \geq 0$,

$$m = 1 + \frac{\nu H\kappa}{3} \quad (45)$$

A procedure similar to that outlined previously in sections 3 and 5.1 for the rigid, perfectly plastic and rigid, strain-rate sensitive cases will be adopted here in order to simplify the constitutive equation (43) for a rigid, strain-hardening material. It is now assumed, therefore, that a linearized yield curve illustrated in Fig. 4(b) will grow as indicated so that the side A'B' is described by equation (44) with $0 \leq m \leq 1$, while (45), with $0 \leq n \leq 1$, defines the behavior of side C'D'.

5.3 Combined Strain-Rate Sensitivity and Strain Hardening

Symonds [14] and Perrone [22] suggested that

$$\frac{\sigma}{\sigma_0} = f(\dot{\epsilon}) g(\epsilon) \quad (46)$$

could be used to analyze structures loaded dynamically, where $f(\dot{\epsilon})$ and $g(\epsilon)$ are strain-rate sensitivity and strain-hardening relations, respectively. It is well known that strain-hardening of some materials decreases with increase in strain-rate, and strictly speaking a stress-strain-strain rate law cannot, therefore, be written in the product form of equation (46) with $f(\dot{\epsilon})$ and $g(\epsilon)$ uncoupled. However, in order to retain mathematical simplicity, it is assumed that the combined effect of strain-hardening and strain-rate sensitivity could be considered in the manner suggested by (46), which using (38) and (42) may be rewritten,

$$\frac{\sigma'}{\sigma_0} = \left\{ 1 + \left(\frac{\dot{\epsilon}}{D} \right)^{1/p} \right\} (1 + v\epsilon) \quad (47)$$

Thus, from equations (40, 41, 44, 45, 47) it is evident that, when $\epsilon \geq 0$, $\dot{\epsilon} \geq 0$, $\kappa = 0$, $\dot{\kappa} = 0$ and $0 \leq m \leq 1$, then

$$n = 1 + v\epsilon + \left(\frac{\dot{\epsilon}}{D} \right)^{1/p} + v\epsilon \left(\frac{\dot{\epsilon}}{D} \right)^{1/p} \quad (48)$$

and when $\epsilon = 0$, $\dot{\epsilon} = 0$, $\dot{\kappa} \geq 0$, $\kappa \geq 0$, and $0 \leq n \leq 1$, then

$$m = 1 + \frac{2p}{2p+1} \left(\frac{H\dot{\kappa}}{2D} \right)^{1/p} + \frac{vH\dot{\kappa}}{3} + \frac{2vH\dot{\kappa}p}{3(2p+1)} \left(\frac{H\dot{\kappa}}{2D} \right)^{1/p} \quad (49)$$

6. Influence of Strain-Hardening and Strain-Rate Sensitivity on Impulsively Loaded Beams

In order to examine the influence of strain-hardening, strain-rate sensitivity, and the combined effect of both on the large final deformations of beams, the constitutive equations developed in the previous section will be used to analyze a rigid-plastic beam with axial restraints which is simply supported at pinned ends and loaded with a uniformly distributed impulse.

6.1 Strain-Rate Sensitivity

First Stage

Equations (13) and (14) give

$$\dot{\epsilon} = w'\dot{w}' , \quad \text{and} \quad \dot{\kappa} = -\dot{w}'' . \quad (50)$$

Thus, it may be shown when employing the mechanism of deformation for the rigid, perfectly plastic beam analyzed in section 4.2 that the velocity profile described by equations (21) and (22) is consistent with the yield condition (40), provided the implication of a discontinuity in curvature at the traveling hinge is disregarded.*

Using the velocity profile described by (21), the strain-rate sensitive relation (40), and equation (33) in order to solve the equilibrium equation (29), yields

$$m = 1 , \quad \text{for} \quad 0 \leq x \leq \rho$$

When $\rho \leq x \leq L$, the corresponding equations give

* If it is assumed that the discontinuity of curvature given by the difference of the appropriate derivatives of equations (21) and (22) can be replaced by a continuous change of curvature across an annulus of width $2H$, then it may be shown that

$$P = \frac{3a\Delta}{\lambda} , \quad \text{approximately}$$

where "P" is the ratio of energy dissipated at a traveling hinge during the first stage to the corresponding loss of kinetic energy, and "a" indicates the factor by which "m" is increased according to the strain-rate sensitivity relation given by equation (41).

In order to simplify the analysis, average values have been used for the speed of the traveling hinge and the radius of curvature across the annulus. P , as might be expected has rather large values when λ is small but for a mild steel beam with $L/H = 12$ ($L = 12$ in.) and $\lambda = 100$, $P \approx 0.06$, while for $\lambda = 800$, $P \approx 0.01$.

$$m = \frac{-\mu V_o}{2M_o t_o (L-\rho)^3} \left(\frac{Lx^2}{2} - \frac{x^3}{6} - L\rho x + \frac{\rho^2 x}{2} + \frac{L\rho^2}{2} - \frac{\rho^3}{3} \right) + \frac{2N_o V_o t_o}{M_o} \left\{ \frac{x^2}{2} - \rho x + \frac{\rho^2}{2} + \frac{\rho}{2p+1} \left(\frac{2V_o t_o}{D(L-\rho)} \right)^{1/p} (x - \rho)^{\frac{2p+1}{p}} \right\} + 1 \quad (51)$$

where the condition $m = 1$ and the continuity requirement $[\dot{m}] + \rho[m'] = 0$ have been satisfied at $x = \rho$.

If the beam is simply supported at pinned ends, then the requirement that $m = 0$ at $x = L$ allows equation (51) to be rewritten in the form

$$\frac{8p\alpha}{2p+1} \Delta^{\frac{2p+1}{p}} + 4\Delta^2 + \Delta - \frac{\lambda}{6} = 0, \quad (52)$$

when $\rho = 0$, and where

$$\alpha = \left(\frac{2V_o H}{DL^2} \right)^{1/p} \quad (53)$$

and

$$\Delta = \frac{V_o t_o L^2}{H} = \frac{\delta_1}{H} \quad (54)$$

Second Stage

Humphreys [10] and Florence and Firth [11] have conducted experiments on beams loaded impulsively, from which it is evident that the deflections occurring at the end of the first stage are comparable with the beam depth. It is shown in references [9,23,24] that membrane forces dominate over bending moments when deflections are of the order of the thickness of rigid-plastic beams and plates loaded dynamically. Furthermore, the mechanism of deformation suggested by equations (21) and (22) implies that two-thirds of the initial kinetic energy is dissipated during the first stage, leaving one-third to be dissipated in the final stage.

In view of the foregoing comments, it seems reasonable to consider that the beam behaves as a membrane during the second stage, the equilibrium equation of which may be obtained from (16) with $Q = 0$,

$$w'' = \frac{\mu}{N_o n} \ddot{w} \quad , \quad (55)$$

where from (40)

$$n = 1 + \left(\frac{\dot{\epsilon}}{D}\right)^{1/p} \quad , \quad \text{and} \quad m = 0 \quad . \quad (56)$$

It is shown later, for the rigid, perfectly plastic case, that equation (55) predicts final results almost identical to those of equation (37). In order to simplify the solution of (55) use will be made of Perrone's [20] observations noted previously in section 5.1. Thus, at the end of the first stage when $\rho = 0$, equations (22, 34, 50) give

$$\dot{\epsilon} = \frac{2V_o^2 t_o x}{L} \quad (57)$$

which, when substituted into (56), yields

$$n = 1 + \left(\frac{2V_o^2 t_o x}{DL}\right)^{1/p} \quad , \quad (58)$$

the average value of which is

$$n_R = 1 + \frac{p}{p+1} \left(\frac{2V_o^2 t_o}{D}\right)^{1/p} \quad . \quad (59)$$

It is more convenient to use "y" measured from the left-hand support so that $y = 0$, $2L$ at the supports and $y = L$ at the beam center; and in order to remove the non-linearity arising in (55) due to (58), a solution will be sought using n_R instead of n .

The general solution of (55) may be expressed in the following form,

$$w = \sum_{k=1,3,5}^{\infty} \left\{ G_k \cos \left(\frac{k\pi c_R t}{2L} \right) + J_k \sin \left(\frac{k\pi c_R t}{2L} \right) \right\} \sin \left(\frac{k\pi y}{2L} \right), \quad (60)$$

where $0 \leq y \leq 2L$, and

$$c_R^2 = \frac{N_o n_R}{\mu} \quad (61)$$

At $t = t_1$, equations (31,22) with $\rho = 0$ and a change of variable noted previously become

$$w = V_o t_o (2Ly - y^2) \quad (62)$$

and

$$\dot{w} = \frac{V_o y}{L}, \quad (63)$$

provided $0 \leq y \leq L$.

If an origin of time is chosen as $T = 0$ at $t = t_1$, then it may be shown that equation (60) and its time derivative subject to the initial conditions expressed by equations (62) and (63) yields

$$G_k = \frac{32V_o t_o L^2}{k^3 \pi^3}, \quad \text{for } k = 1, 3, 5, 7, \dots \quad (64)$$

and

$$J_k = \pm \frac{16V_o L}{k^3 \pi^3 c_R}, \quad (65)$$

where

$$J_k > 0, \quad \text{when } k = 1, 5, 9, \dots$$

and

$$J_k < 0, \quad \text{when } k = 3, 7, 11, \dots$$

Now the beam finally comes to rest at $t = T_f$, where $t_f = t_1 + T_f$. Thus, equating the time derivative of (60) to zero and using (64) and (65) gives

$$\sin\left(\frac{k\pi c_R T_f}{2L}\right) = \frac{1}{(1 + 4c_R^2 L^2 t_o^2)^{1/2}} \quad (66)$$

and

$$\cos\left(\frac{k\pi c_R T_f}{2L}\right) = \frac{\pm 2c_R L t_o}{(1 + 4c_R^2 L^2 t_o^2)^{1/2}}, \quad (67)$$

where + sign is to be used when $k = 1, 5, 9 \dots$, and - sign when $k = 3, 7, 11, \dots$

Making use of equations (60, 64, 65, 66, 67) the deflection of the beam at $T = T_f$ and $y = L$ can be expressed in the following form,

$$\frac{w_m}{H} = \frac{16}{\pi^3} \left(\frac{\lambda}{4n_R} + 4\Delta^2\right)^{1/2} \psi, \quad (68)$$

where

$$\psi = \sum_{k=1,3,5}^{\infty} \frac{1}{k^3} \quad (69)$$

and from (59),

$$n_R = 1 + \frac{p\alpha\Delta}{p+1}^{1/p} \quad (70)$$

Equation (68) with $\alpha = 0$ reduces to the rigid, perfectly plastic case and predicts final deflections at the center of the beam which when plotted in Fig. 3 are almost coincident with the results of equation (37) for the "upper" bound case. Thus waiving the requirement that m should be continuous with respect to time between the two stages of deformation leads to considerable simplification with no concomitant loss of accuracy provided that the L/H ratio of the beam is not too small.

6.2 Strain-Hardening

First Stage

It may be shown that following a procedure somewhat similar to the one outlined in section 6.1 for the strain-rate sensitive case, but using (44) instead of (40), gives

$$4\gamma\Delta^4 + 4\Delta^2 + \Delta - \frac{\lambda}{6} = 0 \quad , \quad (71)$$

where

$$\gamma = v\left(\frac{H}{L}\right)^2 \quad (72)$$

and the implications of a curvature discontinuity at the traveling hinge have been disregarded. In fact, an analysis similar to the one described in the footnote of section 6.1 indicates that P is of the same order of magnitude as in the rate-sensitive case.

Second Stage

It is assumed that the beam behaves like a string throughout the second stage since this simplification for the rigid, perfectly plastic case has been shown previously to lead to final deflections which are almost the same as those predicted by equation (37).

At the end of the first stage, $t = t_1$, and from equations (34) and (44)

$$n = 1 + 2v\frac{V^2 t^2 x^2}{L^2} \quad , \quad (73)$$

the mean value of which is

$$n_H = 1 + \frac{2vV^2 t^2 L^2}{3} \quad (74)$$

If the equilibrium equation (55) was solved using $n = n_H$, then any strain-hardening occurring during the second stage would be disregarded. Thus, in order to consider this additional strain-hardening in an approximate manner, the final strains corresponding to $n = n_H$ will be found by solving equation (55). This then allows a more realistic estimate of n to be made by using the average of the value of n corresponding to this final strain and n_H .

Matching the displacement and velocity of the beam at the end of the first stage to those at the beginning of the second in the manner described previously in section 6.1 gives

$$\bar{w} = \frac{16V_o L}{\pi^3 c_H} (1 + 4c_H^2 L^2 t_o^2)^{1/2} \left[\sum_{k=1,5,9}^{\infty} \frac{\sin(\frac{k\pi y}{2L})}{k^3} - \sum_{k=3,7,11}^{\infty} \frac{\sin(\frac{k\pi y}{2L})}{k^3} \right]$$

and

$$\frac{\partial \bar{w}}{\partial y} = \frac{8V_o}{\pi^2 c_H} (1 + 4c_H^2 L^2 t_o^2)^{1/2} \left[\sum_{k=1,5,9}^{\infty} \frac{\cos(\frac{k\pi y}{2L})}{k^2} - \sum_{k=3,7,11}^{\infty} \frac{\cos(\frac{k\pi y}{2L})}{k^2} \right] \quad (75)$$

when $T = T_f$,

$$c_H^2 = \frac{N_o n_H}{\mu} \quad , \quad (76)$$

and T and y are defined in section 6.1.

The mean final value of strain according to equations (13) and (75) is

$$\bar{\epsilon} = \frac{16V_o^2}{\pi^4} \left(\frac{1}{c_H^2} + 4L^2 t_o^2 \right) \beta \quad , \quad (77)$$

where

$$\beta = \sum_{k=1,3,5,7}^{\infty} \frac{1}{k^4} \quad (78)$$

It is evident from (44) that a membrane force

$$n_F = 1 + v\bar{\epsilon} \quad (79)$$

corresponds to the final strain $\bar{\epsilon}$ given by equation (77) which was derived assuming no strain-hardening during the second stage.

Now, assuming that any strain-hardening during the second stage may be accounted for by taking the average of membrane forces n_H at $T = 0$ ($t = t_1$) and n_F at $T = T_f$ ($t = t_1 + T_f$), then

$$n_A = \frac{n_H}{2} + \frac{1}{2} + \frac{8vV_o^2}{\pi^4} \left(\frac{1}{c_H^2} + 4L^2t_o^2 \right) \beta, \quad (80)$$

which gives, finally

$$\frac{w_m}{H} = \frac{16}{\pi^3} \left(\frac{\lambda}{4n_A} + 4\Delta^2 \right)^{1/2} \psi \quad (81)$$

6.3 Combined Strain-Rate Sensitivity and Strain-Hardening

First Stage

If procedures which were developed for the analyses of the first stages in sections 6.1 and 6.2 are followed, but using equation (48) instead of (40) or (44), then it may be shown that

$$\frac{16p\gamma\alpha}{4p+1} \Delta^{\frac{4p+1}{p}} + \frac{8p\alpha}{2p+1} \Delta^{\frac{2p+1}{p}} + 4\gamma\Delta^4 + 4\Delta^2 + \Delta - \frac{\lambda}{6} = 0 \quad (82)$$

from which the rigid-plastic result and equations (52,71) can be obtained by putting $\alpha = \gamma = 0$, $\gamma = 0$ and $\alpha = 0$, respectively.

Second Stage

If it is assumed that membrane forces alone are important during the second phase of deformation and that strain-rate sensitivity and strain-hardening may be accommodated in the manner described in section 5.3, then

$$\frac{w_m}{H} = \frac{16}{\pi^3} \left(\frac{\lambda}{4n_c} + 4\Delta^2 \right)^{1/2} \psi \quad (83)$$

where

$$n_c = \left(1 + \frac{p\alpha\Delta^{1/p}}{p+1} \right) \left(1 + \frac{\gamma\Delta^2}{3} + \frac{2\gamma\lambda\beta}{\pi^4 n_o} + \frac{32\beta\gamma\Delta^2}{\pi^4} \right) \quad (84)$$

and

$$n_o = \left(1 + \frac{p\alpha\Delta^{1/p}}{p+1} \right) \left(1 + \frac{2\gamma\Delta^2}{3} \right) \quad (85)$$

Equation (83) reduces to the rigid, perfectly plastic case and equations (68) and (81) when $\alpha = \gamma = 0$, $\gamma = 0$ and $\alpha = 0$, respectively.

Discussion

It is clearly evident from Fig. 5, which is plotted using values from equation (68) for the strain-rate sensitive case, that it is important to include strain-rate effects when estimating the permanent deformations of beams loaded impulsively. It is interesting to note for given values of the impulse parameter λ , L/H ratio, and material properties, that the maximum deflection-to-thickness ratio is smaller for smaller beams. This "size effect," which has been noted previously by Symonds [14] and others and follows from the form of equations (52) and (53), is indicated in the Appendix.

Fig. 6, which illustrates the influence of strain-hardening given by equation (81), shows that strain-hardening is particularly important for beams having small L/H ratios.

The results for situations where strain-hardening and strain-rate effects exist simultaneously are given by equation (83) and plotted in Figs. 7-9. These curves indicate that including either strain-hardening alone for beams with small L/H ratios, or strain-rate sensitivity alone for physically small beams, or either for other beams, gives results which compare quite favorably with the combined case. It also appears from Figs. 8 and 9 which are plotted for steel and aluminum beams having the material properties listed in Table I and other calculations that strain-rate sensitivity and strain-hardening are not important for physically large beams having large L/H ratios.

Conclusions

A simple method is herein suggested for estimating the combined influence of strain-hardening and strain-rate sensitivity on the permanent deformation of structures loaded dynamically. In order to assess the predictions of the linearized rigid, strain-rate sensitive, strain-hardening constitutive equation (48), a study has been made of the behavior of a beam which is loaded impulsively and supported at its ends by immovable frictionless pins. It is evident from Figs. 5-9 that when considering strain-hardening alone for beams with small L/H ratios, or strain-rate sensitivity alone

for physically small beams, or either for medium ones, then permanent deflections are predicted which compare rather favorably with those given for the same value of λ by an analysis retaining their combined influence. Moreover, the results suggest that it is not necessary to include either strain-hardening or strain-rate sensitivity for physically large beams having large L/H ratios.

It is not possible to compare the theoretical predictions of this article with experimental results since, to the author's knowledge, no test data have been published for the particular case analyzed. However, it is rather encouraging to note that Humphreys [10] in a study of clamped mild steel beams loaded impulsively recorded permanent deflections which had the same proportion of the values predicted for a rigid, perfectly plastic beam as forecasted here for the corresponding pinned case.

It is thought that the method suggested herein could in principle, at least, be used to analyze beams having other support and loading conditions and extended in order to examine the behavior of plates and shells, though it is felt that some supporting experimental results are required in order to assess the validity, or otherwise, of the various approximations made in the theory.

Acknowledgments

The work reported herein was supported by the Advanced Research Project Agency, Department of Defense, under contract number SD-86 awarded to Brown University.

The author wishes to take this opportunity to express his appreciation to Professor P. S. Symonds for frequent discussions throughout the execution of this work.

Thanks are also due to Miss E. Cerutti for computing the final results and to the National Science Foundation (Grant number GP-4825) for making funds available to cover the costs of machine time.

References

1. Parkes, E. W., "The Permanent Deformation of a Cantilever Struck Transversely at its Tip," Proc. Roy. Soc. London, Vol. 228, Ser. A., 1955, pp. 462-476.
2. Ting, T.C.T., "Large Deformation of a Rigid, Ideally Plastic Cantilever Beam," Jnl. App. Mech., Vol. 32, No. 2, pp. 295-302, 1965.
3. Bodner, S. R., and Symonds, P. S., "Plastic Deformations in Impact and Impulsive Loading of Beams," Plasticity, Pergamon Press, 1960, pp. 488-500.
4. Bodner, S. R., and Symonds, P. S., "Experimental and Theoretical Investigation of the Plastic Deformation of Cantilever Beams Subjected to Impulsive Loading," Jnl. App. Mech., Vol. 29, No. 4, pp. 719-728, 1962.
5. Ting, T.C.T., and Symonds, P. S., "Impact of a Cantilever Beam with Strain-Rate Sensitivity," Proc. 4th U. S. Nat. Cong. App. Mech., pp. 1153-1165, June 1962.
6. Parkes, E. W., "The Permanent Deformation of an Encastred Beam Struck Transversely at Any Point in its Span," Proc. Inst. Civil Engrs., Vol. 10, pp. 277-304, 1958.
7. Lee, E. H., and Symonds, P. S., "Large Plastic Deformations of Beams Under Transverse Impact," Jnl. App. Mech., Vol. 19, No. 3, pp. 308-314, 1952.

8. Manjoine, M. J., "Influence of Rate of Strain and Temperature on Yield Stresses of Mild Steel," *Jnl. App. Mech.*, Vol. 11, pp. 211-218, 1944.
9. Symonds, P. S., and Mentel, T. J., "Impulsive Loading of Plastic Beams with Axial Constraints," *Jnl. Mech. Phys. of Solids*, Vol. 6, pp. 186-202, 1958.
10. Humphreys, J. S., "Plastic Deformation of Impulsively Loaded Straight Clamped Beams," *Jnl. App. Mech.*, Vol. 32, No. 1, pp. 7-10, 1965.
11. Florence, A. L., and Firth, R. D., "Rigid-Plastic Beams Under Uniformly Distributed Impulses," *Jnl. App. Mech.*, Vol. 32, No. 3, pp. 481-488, 1965.
12. Nonaka, T., "Some Interaction Effects in a Problem of Plastic Beam Dynamics," Brown Univ. Report to NSF Grant GP-1115, Div. of Engineering, Dec. 1964.
13. Martin, J. B., and Symonds, P. S., "Mode Approximations for Impulsively-Loaded Rigid-Plastic Structures," *Proc. A.S.C.E.*, Vol. 92, No. EM5, pp. 43-66, 1966.
14. Symonds, P. S., "Viscoplastic Behavior in Response of Structures to Dynamic Loading," *Behavior of Materials Under Dynamic Loading*, Ed. by N. J. Huffington, Publ. by ASME, pp. 106-124, 1965.
15. Witmer, E. A., Balmer, H. A., Leech, J. W., and Pian, T.H.H., "Large Dynamic Deformations of Beams, Circular Rings, Circular Plates, and Shells," *AIAA Jnl.*, Vol. 1, pp. 1848-1857, 1963.
16. Campbell, J. D., and Cooper, R. H., "Yield and Flow of Low-Carbon Steel at Medium Strain Rates," *Proc. Conf. Phys. Basis of Flow and Fract.*, Inst. Physics and Phys. Soc., London, pp. 77-87, 1966.
17. Bodner, S. R., "Strain-Rate Effects in Dynamic Loading of Structures," *Behavior of Metals Under Dynamic Loading*, Ed. by N. J. Huffington, ASME, pp. 93-105, 1965.
18. Cowper, G. R., and Symonds, P. S., "Strain-Hardening and Strain-Rate Effects in the Impact Loading of Cantilever Beams," *Tech. Report No. 28, O.N.R., Contract Nonr-562(10), NR-064-406, Div. of App. Math., Brown Univ.*, Sept. 1957.
19. Wierzbicki, T., "Dynamics of Rigid Viscoplastic Circular Plates," *Arch. Mech. Stos.*, Vol. 17, No. 6, pp. 851-868, 1965.
20. Perrone, N., "On a Simplified Method for Solving Impulsively Loaded Structures of Rate-Sensitive Materials," *Jnl. App. Mech.*, Vol. 32, No. 3, pp. 489-492, 1965.

21. Perrone, N., "Impulsively Loaded Strain-Rate-Sensitive Plates," Jnl. App. Mech., Vol. 34, No. 2, pp. 380-384, 1967.
22. Perrone, N., "A Mathematically Tractable Model of Strain-Hardening, Rate-Sensitive Plastic Flow," Jnl. App. Mech., Vol. 33, No. 1, pp. 210-211, 1966.
23. Jones, N., "Impulsive Loading of a Simply Supported Rigid-Plastic Circular Plate," Brown Univ. Report No. 37 to ARPA, Feb. 1967, accepted for publication, Jnl. App. Mech.
24. Jones, N., "Finite Deflections of a Simply Supported Rigid-Plastic Circular Plate Loaded Dynamically," Brown Univ. Report No. E42 to ARPA, May 1967.

Appendix

Size Effect

$\lambda = \text{constant}$

Consider two beams each of unit width which have the same material properties ρ , D , p , σ_o and L/H ratio and λ but different V_o , L , and H .

$$\text{Now, from equation (28) } \lambda = \frac{4\mu V_o^2 L^2}{\sigma_o H^3} = \frac{4\rho V_o^2 L^2}{\sigma_o H^2} \quad (i)$$

Thus if $\lambda_1 = \lambda_2$ and $L_1/H_1 = L_2/H_2$, then

$$V_{o1} = V_{o2} \quad (ii)$$

Also
$$\alpha = \left(\frac{2V_o H}{DL^2} \right)^{1/p},$$

hence,
$$\left(\frac{\alpha_1}{\alpha_2} \right)^p = \frac{V_{o1} L_2}{V_{o2} L_1}, \quad (iii)$$

which using (ii) becomes

$$\left(\frac{\alpha_1}{\alpha_2} \right)^p = \frac{H_2}{H_1}, \quad (iv)$$

i.e., if $\alpha_2 > \alpha_1$, then $H_2 < H_1$. It is evident from Figs. 5 and 7-9 that smaller deflection-to-thickness ratios are obtained as α increases for a given value of λ . Thus, physically smaller beams are more sensitive to strain-rate sensitivity than larger ones.

Table I

Material	σ_0 , psi	μ/H lb sec ² /in ⁴	ν	D, sec ⁻¹	ρ
Mild Steel	30 000	0.000732	6	40.4	5
Aluminum 6061-T6	40 000	0.000253	2.85	6500	4

Titles of Figures

- Figure 1 - (a) Deformed Shape of Mid-Plane.
(b) Curvature of Beam.
(c) Forces and Moments Acting on an Element of the Beam.
- Figure 2 - Yield Conditions for a Rigid, Perfectly Plastic Material.
- Figure 3 - Impulsive Loading of a Simply Supported Rigid-Plastic Beam with Axial Restraints.
- Figure 4 - (a) Rigid, Strain-Rate Sensitive Yield Condition.
(b) Rigid, Strain-Hardening Yield Condition.
- Figure 5 - Size Effects for Constant λ in Impulsively Loaded Beams which are Made from a Strain-Rate Sensitive Material and Restrained Axially.
- Figure 6 - Influence of Strain-Hardening Alone.
- Figure 7 - Combined Influence of Strain-Hardening and Strain-Rate Sensitivity.
- Figure 8 - Combined Influence of Strain-Hardening and Strain-Rate Sensitivity for Mild Steel Beams with the Material Characteristics Listed in Table I.
- Figure 9 - Combined Influence of Strain-Hardening and Strain-Rate Sensitivity for Aluminum 6061-T6 Beams with the Material Characteristics Listed in Table I.

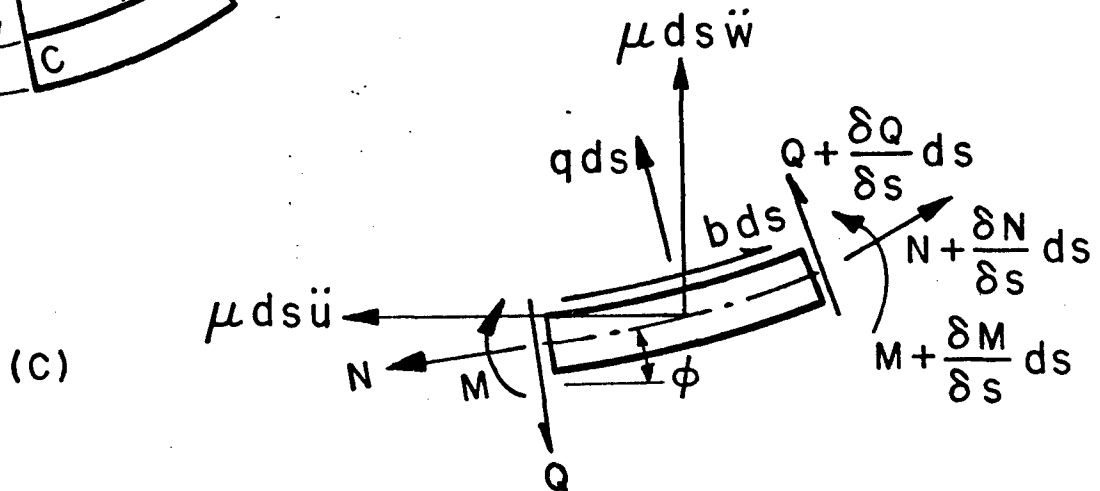
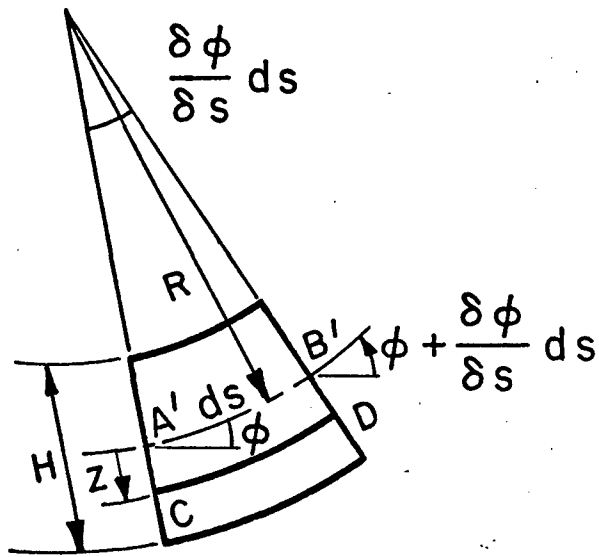
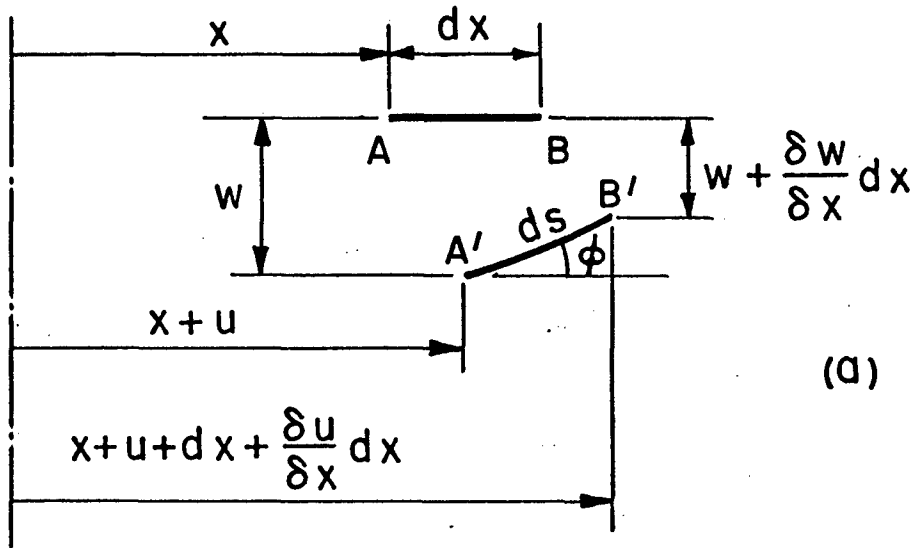


FIG. I

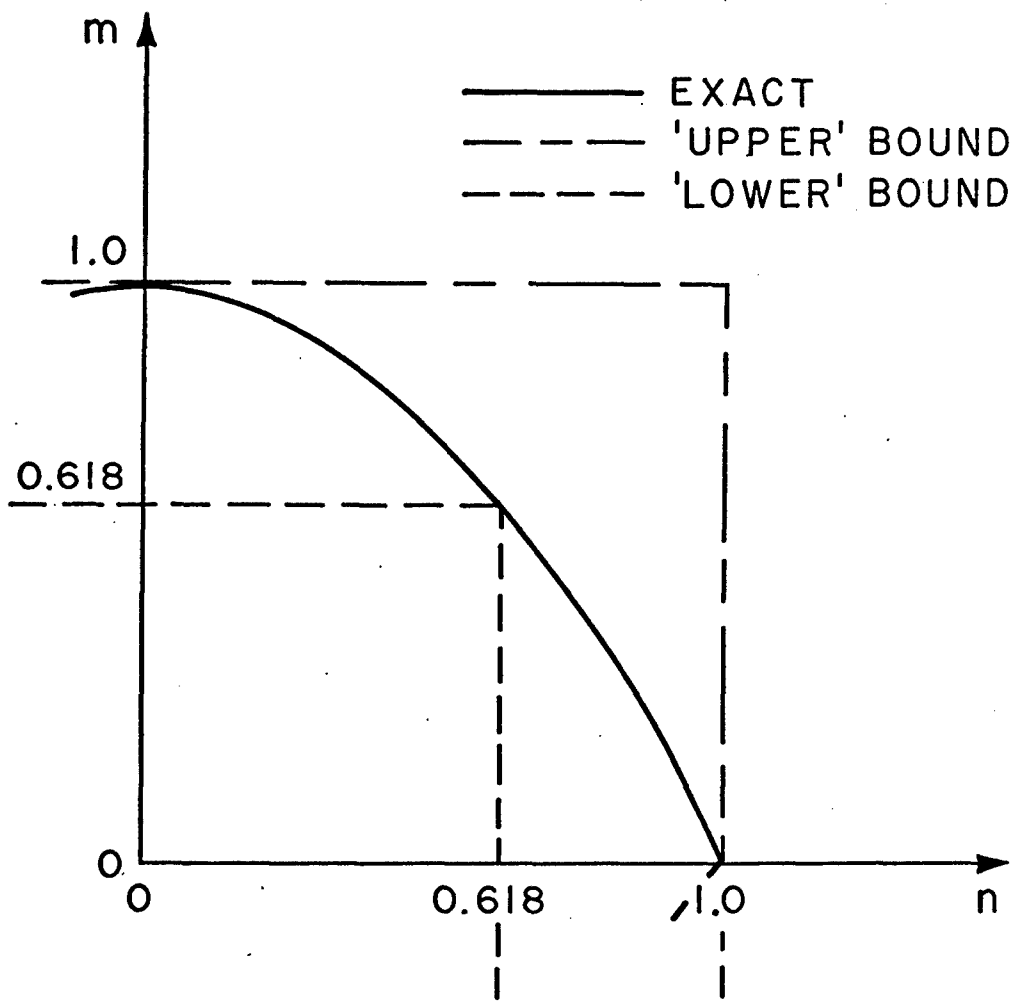
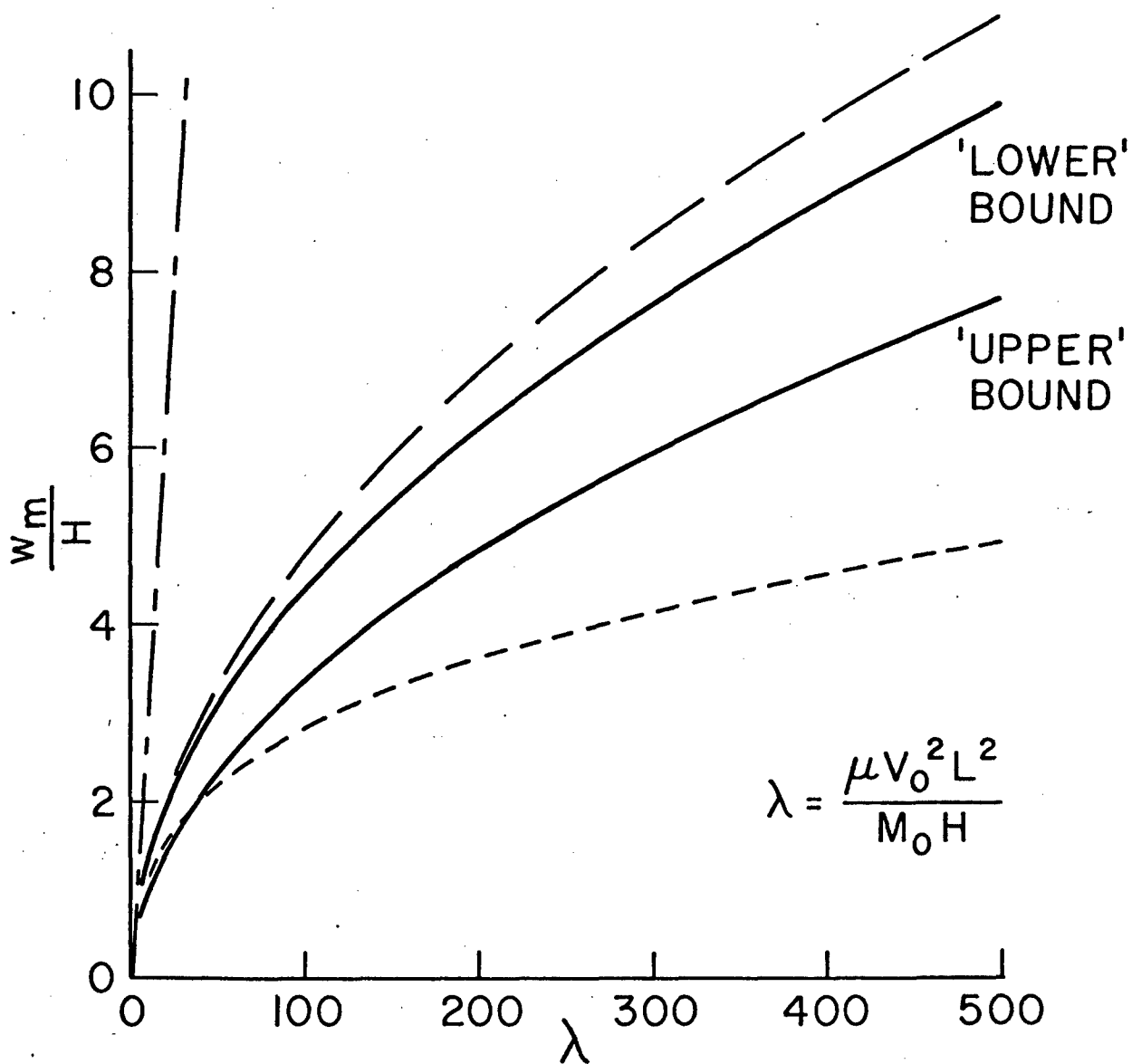


FIG. 2



- — — EQUATION (27) SIMPLE BENDING THEORY
- — — EQUATION (59) OF REF. [9] INCLUDES STRING PHASE
- - - - EQUATION (25) OF REF. [9] EXCLUDES STRING PHASE
- — — EQUATION (37) APPROXIMATE YIELD CURVE

FIG. 3

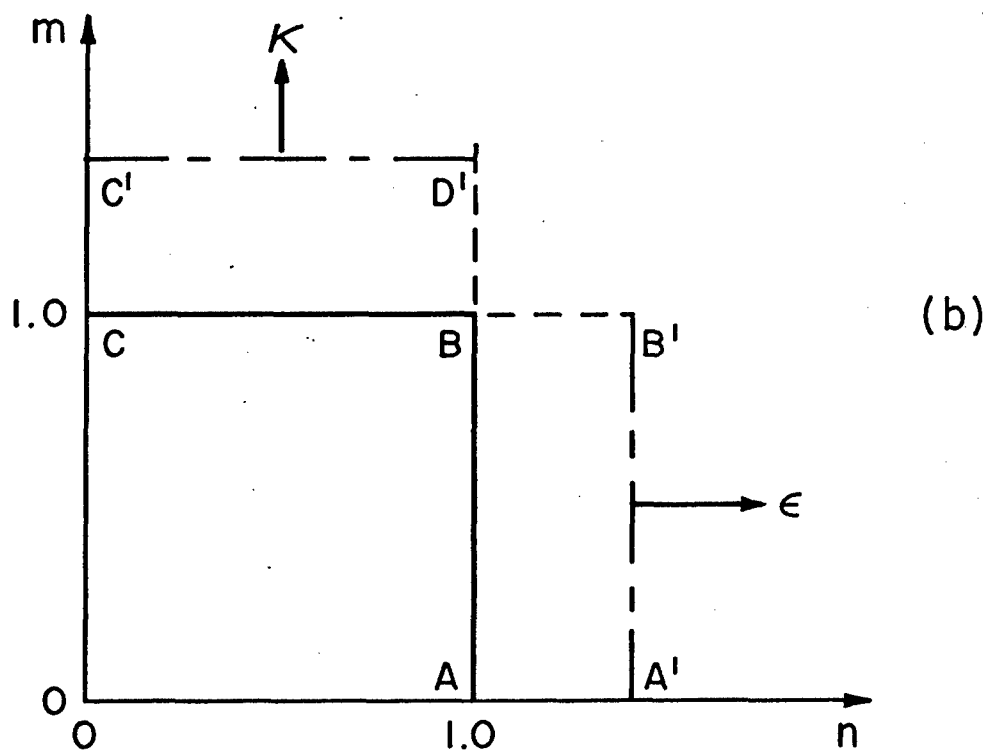
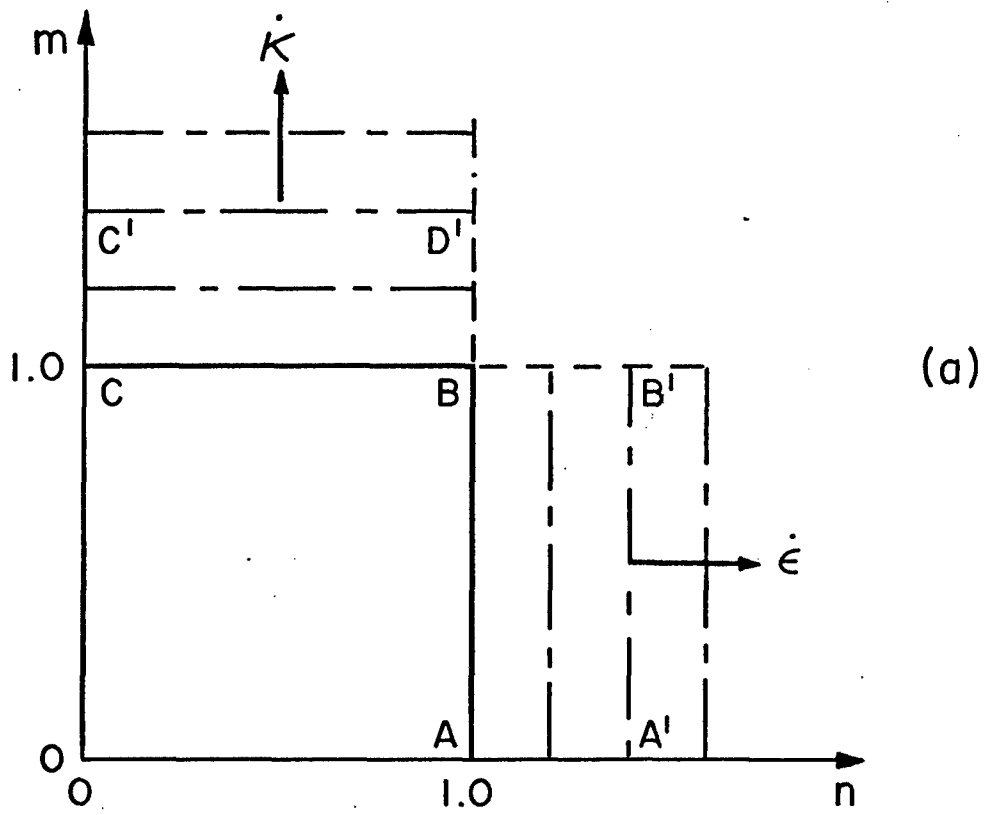


FIG. 4

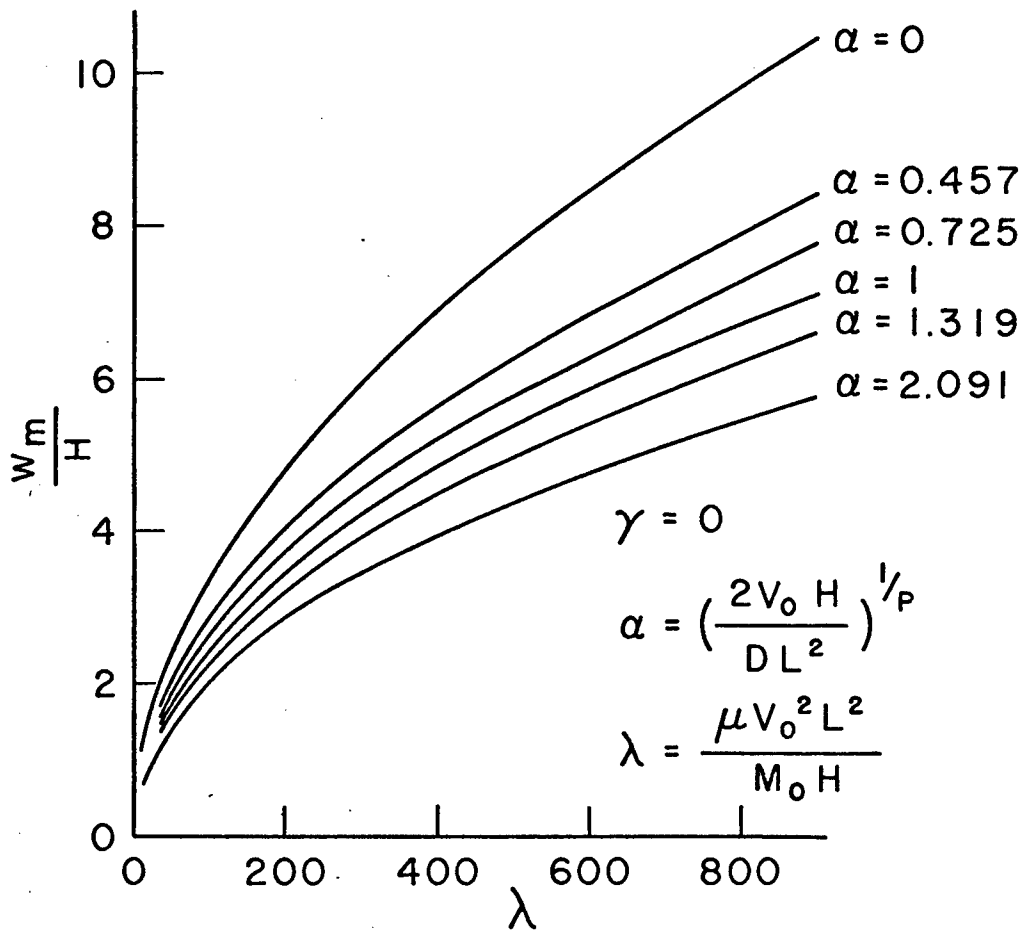


FIG. 5

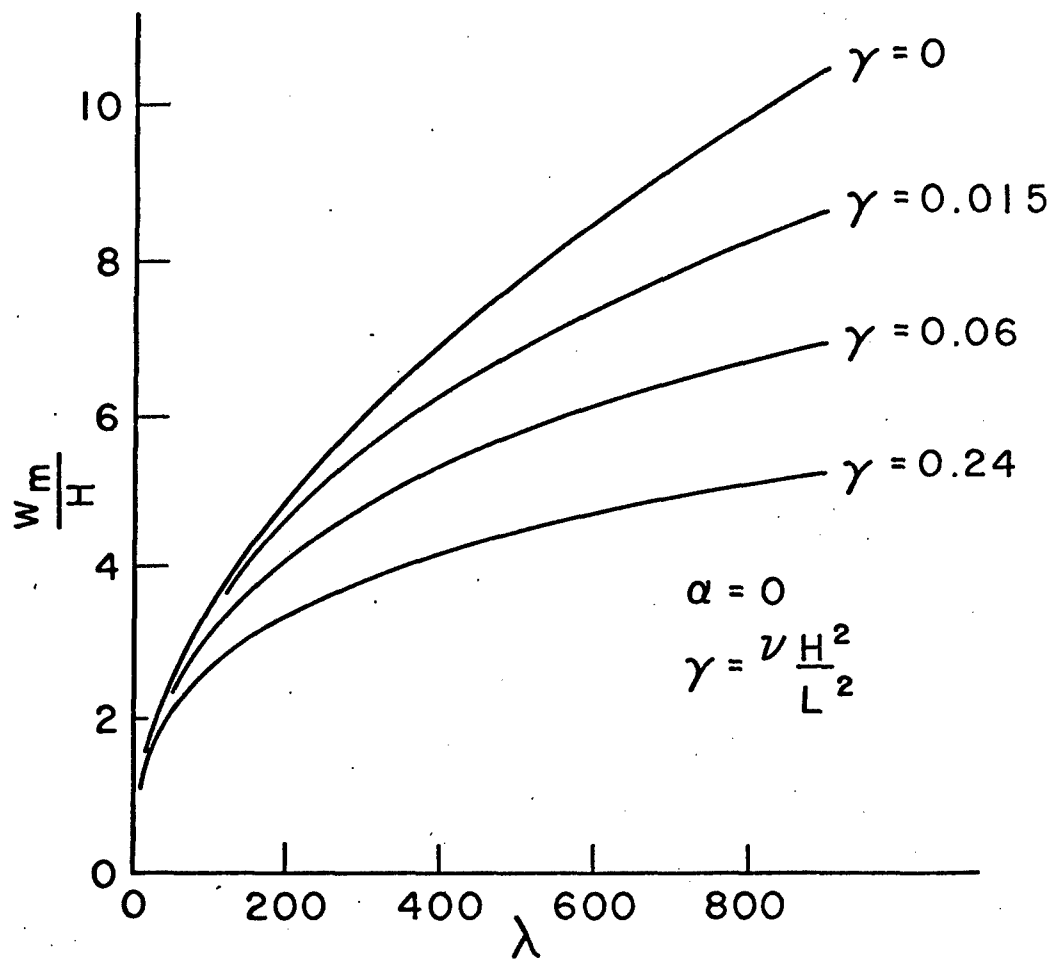


FIG. 6

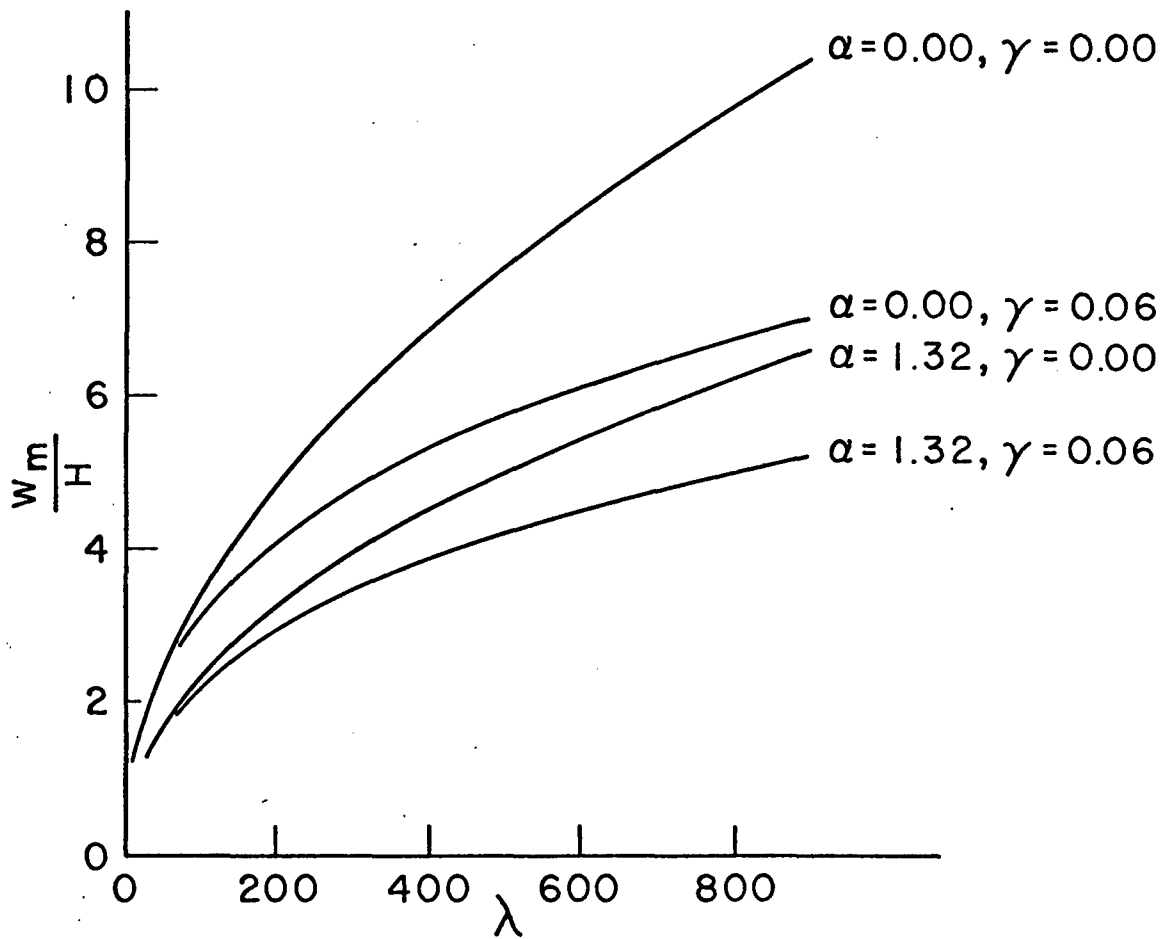


FIG. 7

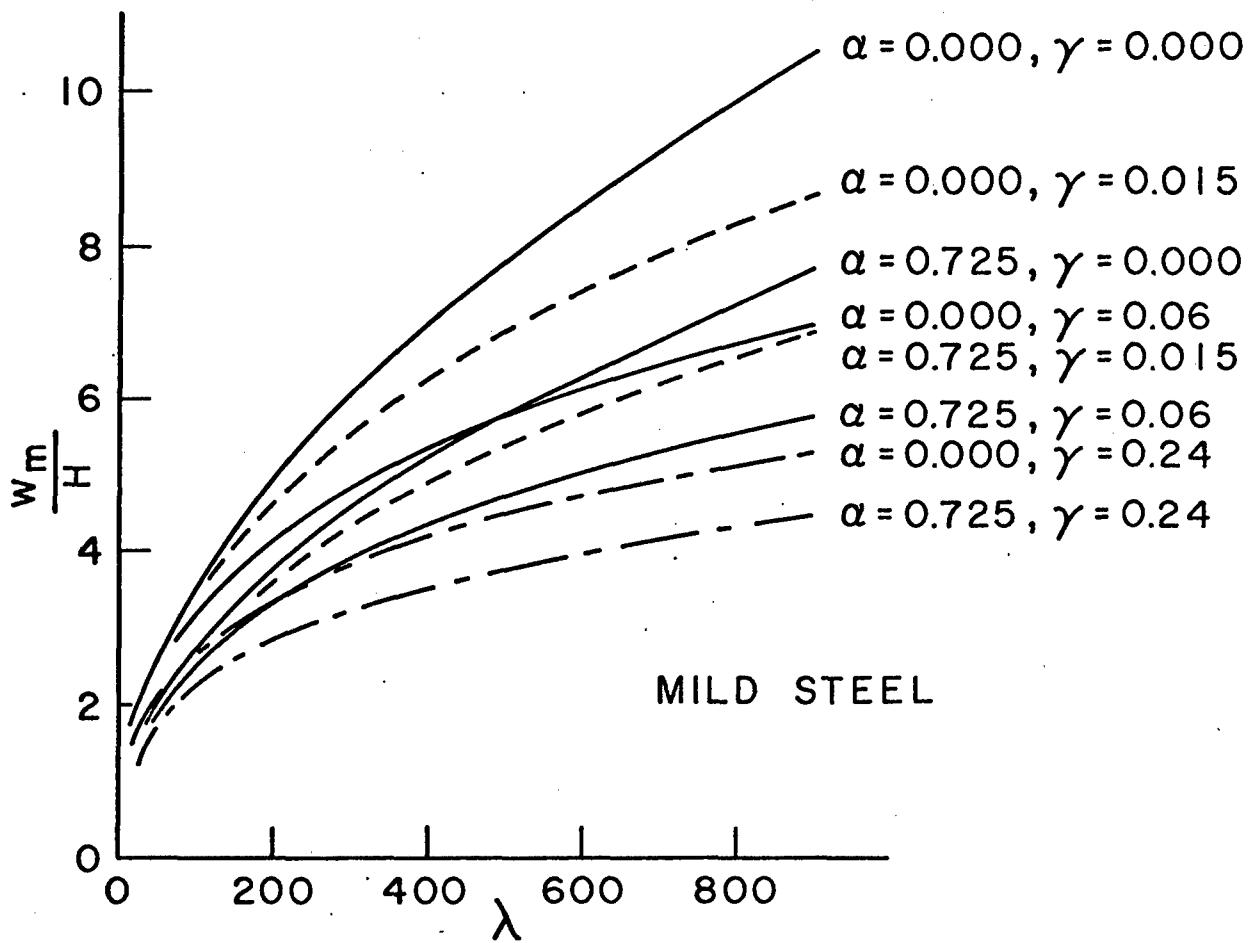


FIG. 8

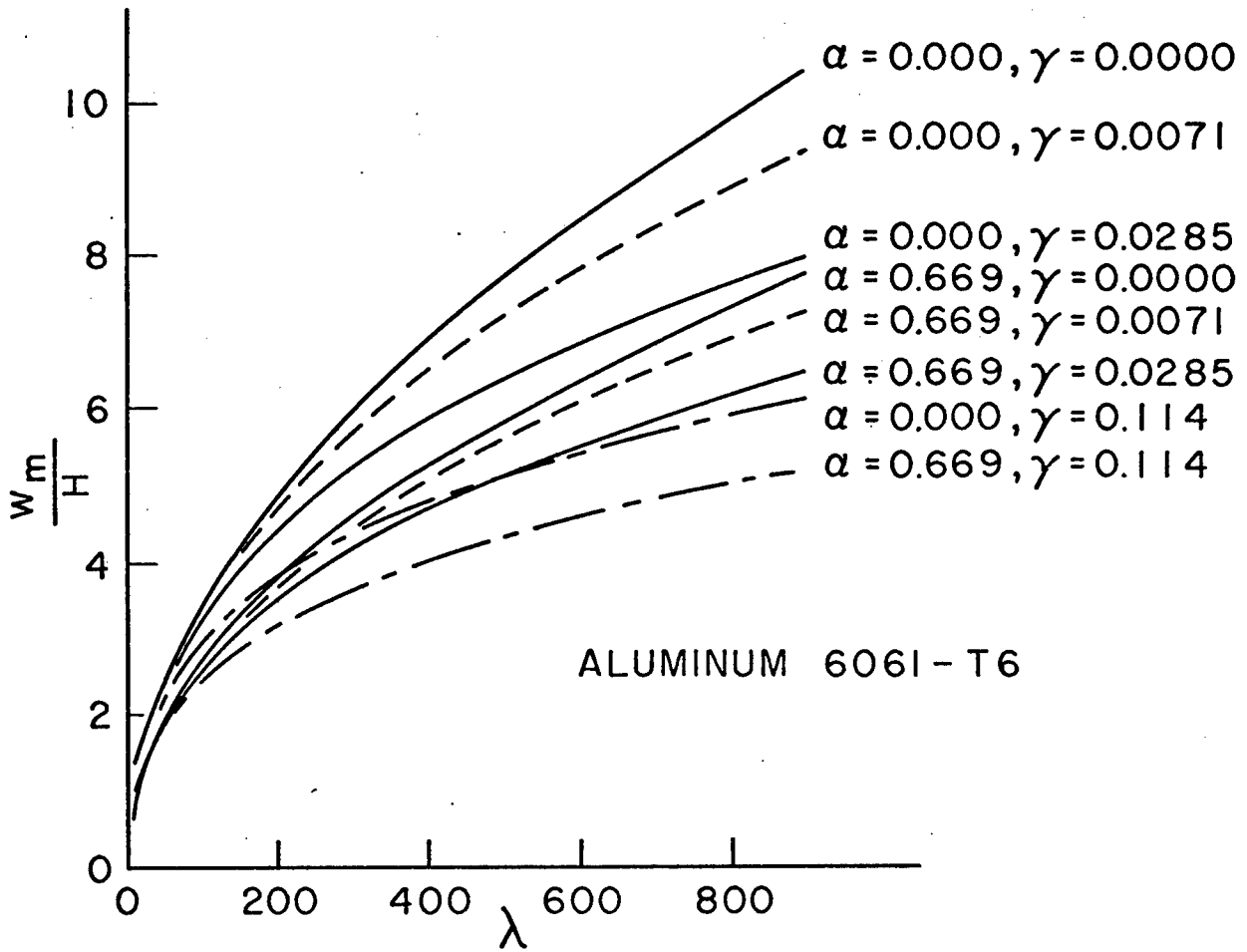


FIG. 9